Angle–angular-momentum entropic bounds and optimal entropies for quantum scattering of spinless particles

D. B. Ion and M. L. D. Ion
National Institute for Physics and Nuclear Engineering Horia Hulubei, P.O. Box MG-6, Bucharest, Romania
(Received 18 February 1999)

In this paper the *angle–angular-momentum entropic lower and upper bounds* are proved by using Tsallis-like entropies, the Riesz theorem, and the Lagrange multiplier method for the quantum scattering of the spinless particles. A connection between optimal states and the most stringent entropic bounds on Tsallis-like entropies in the quantum scattering is established. The results of experimental tests of the *state-independent angle–angular-momentum entropic bounds* as well as of the stringent entropic optimal bounds in pion-nucleus scattering are obtained by calculations of the scattering entropies from the experimental available pion-nucleus *phase shifts*. Comparisons of these results with predictions of the *principle of minimum distance in the space of states* are presented. Then it is shown that experimental pion-nucleus entropies are well described by optimal entropies, and that the experimental data are consistent with the *principle of minimum distance in the space of scattering states*. [S1063-651X(99)08011-3]

PACS number(s): 05.30.−d

I. INTRODUCTION

Over the past two decades there has been an increasing interest [1] in the investigation of quantum entropy. Many authors (see, e.g., Refs. [2–5]) have reviewed the essential properties of various entropy expressions useful in physics. The axiomatic derivation of the Jaynes *principle of maximum entropy* [6], as well as of the Kullback *principle of minimum cross-entropy* [7], were presented in Ref. [8]. Moreover, the *entropic uncertainty relations* [9], which are saturated for coherent states, were proved by many authors (see, e.g., Refs. [1,10]). All these results on the quantum entropy were specifically designed to be applicable to extensive systems. A generalization of such results to nonextensive systems was proposed by Tsallis in Ref. [11], who defined a new form of entropy (see also Refs. [12–14]). On the other hand, the *principle of minimum distance in the space of states* as well as *optimal states* in the Hilbert space of the scattering amplitudes, which are analogous to the coherent states from the Hilbert space of the wave functions, were introduced in Refs. [15–18]. Therefore, it is natural to investigate a possible connection between optimal state dominance [15] and the saturation of some specific entropic lower or upper bounds for the quantum scattering of spinless particles.

In this paper the angle–angular-momentum entropic lower bounds [10] are investigated in a more general form in Sec. II by introducing *Tsallis-like entropies* for the quantum scattering of spinless particles. Hence by using the *Lagrange multiplier method* and the *Riesz theorem* [19], the stringent entropic inequalities as well as the *state-independent angle–angular-momentum entropic lower bounds* are proved in Sec. III for the quantum scattering of spinless particles. The optimal entropies obtained from the *principle of minimum distance in the space of states* [15] are presented in Sec. IV. The results of the experimental tests of the *state-independent angle–angular-momentum entropic bounds* as well as of the stringent entropic optimal bounds in pion-nucleus scattering are obtained in Sec. V by calculations of the scattering entropies from the experimental available *phase shifts* [20–24]. Comparisons of these results with predictions of the *principle of minimum distance in the space of states* [15] are also given in Sec. V. Section VI is reserved for discussions and conclusions. A very short version of this paper was published in Ref. [25].

II. INFORMATION ENTROPIES FOR QUANTUM SCATTERING

A. Some basic definitions

We start with a two-body scattering process

$$a+b\to a+b, \tag{1}$$

where, for simplicity, a and b are spin-0 hadrons, and $x=\cos\theta$, θ being the center of mass scattering angle. Let $f(x), x\in[-1,1]$ be the scattering amplitude of the two-body scattering process (1). As is well known, if the normalization of $f(x)$ is chosen such that the differential cross section $(d\sigma/d\Omega)(x)$ is given by

$$\frac{d\sigma}{d\Omega}(x)=|f(x)|^2,\quad x\in[-1,1], \tag{2}$$

then the elastic integrated cross section σ_{el} is given by

$$\sigma_{\mathrm{el}}=2\pi\int_{-1}^{+1}\frac{d\sigma}{d\Omega}(x)dx=2\pi\int_{-1}^{+1}|f(x)|^2dx=2\pi\|f\|^2. \tag{3}$$

Since we will work at a fixed energy, the dependence of σ_{el} and $(d\sigma/d\Omega)(x)$ and $f(x)$ on this variable was suppressed.

Now let H be the Hilbert space of the scattering states, defined on the interval $S\equiv[-1,1]$, with the inner product $\langle\cdots\rangle$ and the norm $\|\cdot\|$ given by

$$\langle f,g\rangle=\int_{-1}^{+1}f(x)\overline{g(x)}dx,\quad f,g\in H, \tag{4}$$

 © 1999 The American Physical Society

$$\|f\|^2=\langle f,f\rangle=\int_{-1}^{+1}|f(x)|^2dx, \quad f\in H. \tag{5}$$

B. Angular entropy S_θ

The informational angular entropy S_θ of any quantum scattering states is defined as in Ref. [10] by

$$S_\theta=-\int_{-1}^{1}dxP(x)\ln P(x), \tag{6}$$

where $P(x)$ is the angular distribution defined in terms of the differential cross section by

$$P(x)=\frac{2\pi}{\sigma_{\rm el}}\frac{d\sigma}{d\Omega}(x), \quad \int_{-1}^{1}P(x)dx=1\,. \tag{7}$$

The quantum entropy S_θ [Eq. (7)] was specifically designed to be applicable to extensive scattering systems [Eq. (1)]. Generalization of this entropy to the nonextensive scattering can be obtained by defining a kind of entropy similar to that proposed by Tsallis in Ref. [11] (see also Refs. [12–14]). Hence we define the Tsallis-like angular entropies as follows:

$$S_\theta(q)=\frac{1}{q-1}\left\{1-\int_{-1}^{1}dx[P(x)]^q\right\}, \quad q\in R, \tag{8}$$

with the property

$$\lim_{q\to1} S_\theta(q)=S_\theta(1)=S_\theta. \tag{9}$$

C. Angular-momentum entropy S_L

Now let us consider the case when the scattering amplitude $f(x)$ of the spinless particles is developed in partial amplitudes as

$$f(x)=\sum_{l=0}^{L}(2l+1)f_lP_l(x), \quad x\in[-1,1], \quad f_l\in C, \tag{10}$$

where $L+1$ is the number of partial amplitudes f_l, and $P_l(x)$, $l=0,1,\ldots,L$, are Legendre polynomials. Then the Fourier coefficients, or the partial amplitudes f_l, are expressed as

$$f_l=\frac{1}{2}\int_{-1}^{+1}f(x)P_l(x)dx, \quad f_l\in C. \tag{11}$$

Hence, as in Ref. [10] we define the angular-momentum entropy S_L by

$$S_L=-\sum_{l=0}^{L}(2l+1)p_l\ln p_l, \tag{12}$$

where the partial probability p_l are defined by

$$p_l=4\pi\frac{|f_l|^2}{\sigma_{\rm el}}, \quad \sum_{l=0}^{L}(2l+1)p_l=1. \tag{13}$$

Of course, in this case, the Tsallis-like angular-momentum entropies for the scattering process can be defined as

$$S_L(q)=\frac{1}{q-1}\left\{1-\sum_{l=0}^{L}(2l+1)[p_l]^q\right\}, \quad q\in R, \tag{14}$$

with the property

$$\lim_{q\to1} S_L(q)=S_L(1)=S_L\,. \tag{15}$$

D. Angle–angular-momentum entropy $S_{\theta L}$

The entropies (6) and (12) are defined as natural measures of the uncertainties corresponding to the distributions of probabilities $P(x)$ and p_l, respectively. If we are interested in obtaining a measure of uncertainty of the simultaneous realization of the probability distributions $P(x)$ and p_l, then we must calculate the entropy corresponding to the product of these distributions: $P(x,l)=P(x)p_l$. It is easy to verify that the angle–angular-momentum entropy is given by

$$S_{\theta L}=-\sum_{l=0}^{L}(2l+1)\int_{-1}^{1}dxP(x,l)\ln[P(x,l)]=S_\theta+S_L\,. \tag{16}$$

In this case the Tsallis-like entropies for the scattering of spinless particles is given by

$$\begin{aligned}S_{\theta L}(q)&=\frac{1}{q-1}\left(1-\sum_{l=0}^{L}(2l+1)p_l^q\int_{-1}^{1}dx[P(x)]^q\right)\\&=S_\theta(q)+S_L(q)+(1-q)S_\theta(q)S_L(q), \quad q\in R,\end{aligned} \tag{17}$$

with the property

$$\lim_{q\to1} S_{\theta L}(q)=S_{\theta L}(1)=S_{\theta L}=S_\theta+S_L\,. \tag{18}$$

Therefore, the index $q\neq1$ controls the degree of entropy nonextensivity reflected in the pseudoadditivity entropy rule (17).

III. ENTROPIC INEQUALITIES

A. Angular entropic inequalities

It is interesting here to present the following generalized entropic inequalities for the Tsallis-like entropies for the scattering of spinless particles:

$$\frac{1}{q-1}[1-K^{q-1}(1,1)]\leqslant S_\theta(q)\leqslant\frac{1}{q-1}[1-2^{1-q}] \quad \text{for } q>0 \tag{19}$$

and

$$\frac{1}{q-1}[1-2^{1-q}]\leqslant S_\theta(q) \quad \text{for } q<0. \tag{20}$$

The proof of the lower bound (19) is provided by considering the condition that $P(x)$ has, everywhere, a finite magnitude, i.e.,

$$P(x) \leqslant P(1) = K(1,1) = \frac{1}{2}(L_o+1)^2 = \frac{2\pi}{\sigma_{\rm el}}\frac{d\sigma}{d\Omega}(1). \tag{21}$$

The upper bound (19) as well as the lower bound (20) are optimal bounds which can be obtained via Lagrange multipliers by extremizing the Tsallis-like entropies subject to the normalization constraints (7) and (13), respectively.

B. Angular-momentum entropic inequalities

Here the following generalized entropic inequalities for the Tsallis-like entropies for the scattering of spinless particles are proved:

$$S_L(q) \leqslant \frac{1}{q-1}[1-[L+1]^{2(1-q)}] \quad \text{for} \quad q>0, \tag{22}$$

$$\frac{1}{q-1}[1-[L+1]^{2(1-q)}] \leqslant S_L(q) \quad \text{for} \quad q<0. \tag{23}$$

Next, the upper bound (22) as well as the lower bound (23) are optimal bounds which can be obtained via Lagrange multipliers by extremizing the Tsallis-like entropies subject to the normalization constraint (13), respectively.

Indeed, as an example, here we prove bounds (22) and (23) via Lagrange multipliers, starting with

$$\pounds(p_l) = \frac{1}{q-1}\left\{1-\sum_{l=0}^{L}(2l+1)[p_l]^q\right\} + \lambda\left\{1-\sum_{l=0}^{L}(2l+1)p_l\right\} \to (\text{extremum}), \tag{24}$$

where $\lambda \in R$ is a Lagrange multiplier. Then, for extremum (maximum and minimum), we have

$$\frac{\partial \pounds}{\partial p_l} = -\frac{q}{q-1}(2l+1)p_l^{q-1} - \lambda(2l+1) = 0,$$
$$\frac{\partial^2 \pounds}{\partial p_l \partial p_{l'}} = -q(2l+1)p_l^{q-2}\delta_{ll'} \lesseqgtr 0. \tag{25}$$

Therefore, we obtain that the solution of Eqs. (18) is given by the maximum-entropy distribution

$$\{p_l^{me} = [L+1]^{-2}, \quad l=0/L\}, \tag{26}$$

in both cases $q>0$ and $q<0$.

As we see from Eq. (25),

$$\frac{\partial^2 \pounds}{\partial p_l \partial p_{l'}} < 0 \quad \text{for} \quad q>0$$

and

$$\frac{\partial^2 \pounds}{\partial p_l \partial p_{l'}} > 0 \quad \text{for} \quad q<0.$$

Hence for $q>0$ we obtain the entropic upper bound (20), while for $q<0$ we obtain the entropic lower bound (22). In conclusion, the equality holds in the upper bound (20) and lower bound (22) if and only if $\{p_l, l=0/L\}$ in Eq. (12) is the maximum-entropy distribution (26).

C. State-independent angle–angular-momentum entropic lower bound

Here we prove the state-independent entropic lower bound

$$\ln 2 \leqslant S_\theta + S_L. \tag{27}$$

A general proof of Eq. (27) can be obtained by applying the Riesz theorem (see theorem 2.8 from Ref. [19], p. 102). Indeed, by using the relations

$$\left[\int P^m(x)dx\right]^{1/2m} = [1+(1-m)S_\theta(m)]^{1/2m}$$
$$\left[\sum (2l+1)p_l^m\right]^{1/2m} = [1+(1-m)S_L(m)]^{1/2m}, \quad m=p,q \tag{28}$$

from the *theorem 2.8* (of Ref. [19]), (with $p \to 2p$ and $p' \to 2q$, so that $p^{-1}+q^{-1}=2$), we obtain the following general result.

State-independent (p,q) *entropic bound:* (i) Let $f \in L^p(-1,+1), \frac{1}{2}<p\leqslant 1$, be the scattering amplitude satisfying Eq. (10) with the Fourier coefficients given by Eq. (11). If the scattering Tsallis-like entropies are defined by Eqs. (8) and (14), respectively, then the entropic inequality

$$[1+(1-q)S_L(q)]^{1/2q} \leqslant \exp\left\{\left[\frac{p-1}{2p}\right]\ln 2\right\}[1+(1-p)S_\theta(p)]^{1/2p} \tag{29}$$

hold for any q defined by the relation $(1/2p)+(1/2q)=1$.

(ii) For any finite sequence f_l with finite $[1+(1-p)S_L(p)]^{1/2p}$ there is an $f \in L^q(-1,+1)$ satisfying Eq. (10), for which

$$[1+(1-q)S_\theta(q)]^{1/2q} \leqslant \exp\left\{\left[\frac{p-1}{2p}\right]\ln 2\right\}[1+(1-p)S_L(p)]^{1/2p}, \tag{30}$$

where $(1/2p)+(1/2q)=1$. Hence, in the limit $p\to 1$ and $q \to 1$, from Eq. (29) [or from Eq. (30)], by developing in powers of $\Delta p(\Delta q = -q^2\Delta p/p^2)$ and considering only the first terms, we obtain the lower bound (27).

IV. OPTIMAL ENTROPIES

A. Principle of minimum distance in the space of states

It is well known that any optimizing study [34] ideally involves three steps: (i) The description of the system, by which one should know, accurately and quantitatively, the variables of the system as well as how these system variables interact. (ii) Finding a unique measure of the system effectiveness expressible in terms of the system variables. (iii) The optimization by which one should choose those values of the system variables yielding optimum effectiveness.

In attempting to use the optimization theory for analyzing the interaction of elementary particles, one can reverse the order of these three steps. Then, knowledge of the interacting system can be deduced by assuming that it behaves so as to optimize some given measure of its effectiveness, and thus the behavior of the system is completely specified by identifying the criterion of effectiveness and applying optimization to it. This approach is in fact known as describing the system in terms of an optimum principle. The earliest optimum principle was proposed by Hero of Alexandria (125 B.C.) in his *Catoptrics* in connection with the behavior of light. Thus Hero of Alexandria mathematically proved the following genuine scientific minimum principle of physics (HPMD): *When a ray of light is reflected by a mirror, the path actually taken from the object to the observer's eye is the shortest path from all possible paths.*

Now let us apply the HPMD idea to the behavior of light in gravitational fields. Then we can obtain immediately that according to the HPMD, modified to include the interaction of light with the gravitational field, light must move on a specific shortest path which is the geodesic.

This very simple optimum principle was recently [15] extended to quantum physics by choosing ''partial transition amplitudes'' as fundamental physical quantities with good quantum numbers such as charge, angular momentum, isospin, etc. These physical quantities are chosen as system variational variables, while the distance in the Hilbert space of the quantum states is taken as measure of the system effectiveness expressed in terms of the system variables. The principle of minimum distance in the space of states is chosen as variational optimum principle by which one should obtain those values of the partial amplitudes yielding optimum effectiveness. Then it was shown (see again Ref. [15]) that the predictions based on this new optimum principle can explain the experimental data on hadron-hadron scattering with high accuracy. In a general form this optimum principle can be formulated as follows:

Principle of minimum distance in the space of quantum states (PMD–SQS): If $D(f,g)=\min_{\Phi}\|f-g\exp(-i\Phi)\|=[\|f\|^2+\|g\|^2-2|\langle f,g\rangle|]^{1/2}$ is the quantum distance between two arbitrary states f and g of a giving system and h is the quantum state of the system when the interaction is missing, then the true interacting quantum state f of the interacting system is that state which posses the shortest distance $D(f,h)$ in the space of interacting states compatible with the constraints imposed by the interaction.

Of course this optimum principle, like the PMD-SQS, can be formulated in a more general mathematical form by using the S-matrix theory of the strong interacting systems. Such generalizations, similar to the PMD-SQS, can be made in any branch of science by introducing specific spaces; e.g., in genetics, one can introduce the principle of minimum distance in the genetic space, etc.

Now our purpose is to show how to deduce knowledge about the scattering system [Eq. (1)] by using the (PMD-SQS) [15]. So, the description of the scattering amplitude $f(x)$ of system (1) will be given in terms of partial amplitudes $f_l, l=0,1,\ldots,L$, by formula (10). As system variables we consider the partial amplitudes $f_l, l=0,1,\ldots,L$. Now, since the norm $D(f,0)=\|f\|$ given by Eq. (3) is the natural distance in the space of states, as a unique measure of the system effectiveness we can choose the elastic integrated cross section expressed in terms of the system variables as follows: $\sigma_{\mathrm{el}}/2\pi=2\Sigma(2l+1)|f_l|^2=\|f\|^2$. Then, the behavior of scattering system (1) will be completely specified by the optimal partial amplitudes obtained as the solutions of the constrained minimization problem, i.e.,

$$\min\|f\|, \quad \text{when } \frac{d\sigma}{d\Omega}(y)=\text{fixed}, \quad y\in[-1,1],$$

or equivalently,

$$\min\left\{\sum (2l+1)|f_l|^2 + \alpha\left[\frac{d\sigma}{d\Omega}(y)-\left|\sum (2l+1)f_l P_l(y)\right|^2\right]\right\}, \quad (31)$$

where f_l are the partial amplitudes [see Eqs. (10) and (11)], $P_l(y)$ are the Legendre polynomials, and α is a Lagrange multiplier.

The unique solution of the minimum norm problems of the form of Eq. (31) can be obtained in an elegant and general form by the reproducing kernel Hilbert space (RKHS) method. Therefore, let H be the Hilbert space of the scattering amplitudes defined by the scalar product (4) and norm (5). The Hilbert space H of the scattering states is a RKHS if the following two properties are fulfilled: (i) There exists a complex valued function $K(x,y)$ on $S\times S$, called a reproducing kernel (RK), such that:

$$K_y\in H \quad (32)$$

for any fixed y in $S\equiv[-1,1]$.

(ii) K_y obeys the reproducing property

$$K_y(x)=K(x,y)\Rightarrow\langle f,K_y\rangle=f(y) \quad (33)$$

for each f from H and any y in $S\equiv[-1,1]$. K_y is the reproducing element from point y, while the totality of elements K_y is the RK of the Hilbert space H.

The reproducing kernel was introduced by Aronsjain [26] and Bergman [27]. Its usefulness was demonstrated in many fields of mathematics and physics (see also Refs. [16–18] and [28–31]).

Now we recall briefly some of the definitions and results on optimal states introduced in Refs. [15–18] that are less known and are used in this investigation. The RKHS has the following useful properties.

(i) The RK, if it exists is unique.

(ii) Hermitian symmetry: $K(x,y)=\overline{K(x,y)}$.

(iii) Autoreproducing properties:

$$|K(x,y)|^2\leqslant K(x,x)K(y,y), \quad \|K_y\|^2=K(y,y)\geqslant 0. \quad (34)$$

(iv) If the Hilbert space H of the scattering amplitudes f is a RKHS with a RK denoted by K, then for all f in H and any y in S,

$$|f(y)|\leqslant[K(y,y)]^{1/2}\|f\| \quad \text{or} \quad \frac{d\sigma}{d\Omega}(y)\leqslant\frac{\sigma_{\rm el}}{2\pi}K(y,y), \tag{35}$$

the equality is holding in Eq. (35) if and only if

$$f(x)=f_{oy}(x)=f(y)\frac{K(x,y)}{K(y,y)}, \quad K(y,y)\neq 0\,. \tag{36}$$

(v) If $\{\Phi_n\}$ is a complete orthonormal sequence in RKHS, then the RK is given by

$$K(x,y)=\sum \overline{\Phi}_n(x)\Phi_n(y). \tag{37}$$

Hence, as a corollary of properties (35), we obtain

$$P(y)\equiv\frac{2\pi}{\sigma_{\rm el}}\frac{d\sigma}{d\Omega}(y)\leqslant K(y,y) \tag{38}$$

for any $y\in[-1,1]$ for which the $K(y,y)\neq 0$, the equality in Eq. (38) holding if and only if the scattering amplitude f is the *optimal* scattering amplitude [Eq. (36)]. Therefore, in order to obtain the concrete expression of the optimal state (36) we must calculate the reproducing kernel function $K(x,y)$ corresponding to scattering amplitudes (10). In this case it is easy to verify that (see Ref. [15]) (a) the scattering amplitude $f(x)$ is an element of a RKHS H defined on $[-1,1]$ if and only if $L<\infty$; and (b) H is a finite $(L+1)$-dimensional subspace $L^2[-1,1]$. Then, according to Eq. (37), the Hilbert space H possesses a polynomial reproducing kernel given by

$$\begin{aligned} K(x,y)&=\frac{1}{2}\sum_{l=0}^{L}(2l+1)P_l(x)P_l(y)\\ &=\frac{L+1}{2}\,\frac{P_{L+1}(x)P_L(y)-P_L(x)P_{L+1}(y)}{x-y}, \end{aligned} \tag{39}$$

$$\begin{aligned} K(y,y)&=\frac{1}{2}\sum_{l=0}^{L}(2l+1)P_l(y)P_l(y)\\ &=\frac{L+1}{2}[\dot{P}_{L+1}(y)P_L(y)-\dot{P}_L(y)P_{L+1}(y)], \end{aligned} \tag{40}$$

where $\dot{P}_l(y)\equiv dP_l(x)/dx$.

Indeed, using Eqs. (4) and (10), we can verify that $K(x,y)$ given by Eq. (39) fulfills the reproducing property [Eq. (33)].

$$\begin{aligned} \langle f,K_y\rangle&=\int_{-1}^{+1}dx\left\{\sum (2l+1)f_{l'}P_{l'}(x)\right\}\\ &\quad\times\left\{\frac{1}{2}\sum (2l+1)P_l(x)P_l(y)\right\}\\ &=\sum (2l+1)f_lP_l(y)=f(y), \end{aligned}$$

since

$$\int_{-1}^{+1}dx\,P_l(x)P_{l'}(x)=[2/(2l+1)]\delta_{ll'}\,.$$

In the particular case $y=1$ we have the following important results (see again Ref. [15]). If $\sigma_{\rm el}$ and $d\sigma/d\Omega(1)$ are fixed from experiment, then the number $(L+1)$ of partial amplitudes, in any phase shift analysis must obey the optimal bound

$$(L+1)^2\geqslant\frac{4\pi}{\sigma_{\rm el}}\frac{d\sigma}{d\Omega}(1), \tag{41}$$

or, equivalently,

$$L+1\geqslant L_o+1=\text{integer}\times\left\{\left[\frac{4\pi}{\sigma_{\rm el}}\frac{d\sigma}{d\Omega}(1)\right]^{1/2}\right\}. \tag{42}$$

The equality in Eq. (41) holds if and only if $f(x)$ is equal to the optimal state [Eq. (36)] for $y=1$, which now is given as

$$f_{o1}(x)=f(1)\frac{K(x,1)}{K(1,1)}=f(1)\frac{\dot{P}_{L+1}(x)+\dot{P}_L(x)}{(L+1)^2}, \tag{43}$$

with $L=L_o$, respectively.

We note that the model-independent result [Eq. (41)] includes, in a more general and exact form, the Rarita-Schwed bound (see Ref. [32])

$$(L+1)^2\geqslant\sigma_T^2/4\pi\bar{\lambda}^2\sigma_{\rm el}\,,$$

and also the bound

$$(L+1)^2\geqslant\sigma_T/4\pi\bar{\lambda}^2.$$

B. Optimal angular entropy

Now, having obtained the concrete optimal states, the optimal angular entropy S_θ^{oy}, as well as the corresponding Tsallis entropy $S_\theta^{oy}(p)$, are given by

$$S_\theta^{oy}=-\int_{-1}^{1}\frac{[K(x,y]^2}{K(y,y)}\ln\frac{[K(x,y]^2}{K(y,y)}dx \tag{44}$$

and

$$S_\theta^{oy}(p)=\frac{1}{p-1}\left\{1-\int_{-1}^{1}dx\left[\frac{[K(x,y]^2}{K(y,y)}\right]^p\right\}, \quad p\in R, \tag{45}$$

since

$$P^{oy}(x)=\frac{[K(x,y)]^2}{K(y,y)}, \quad \int_{-1}^{1}\frac{[K(x,y)]^2}{K(y,y)}dx=1. \tag{46}$$

C. Optimal angular-momentum entropy

The optimal angular entropy S_θ^{oy}, as well as the corresponding Tsallis entropy $S_\theta^{oy}(q)$, are given by

$$S_L^{oy} = -\sum (2l+1)\frac{P_l^2(y)}{2K(y,y)}\ln\left[\frac{P_l^2(y)}{2K(y,y)}\right]$$
$$= \ln[2K(y,y)] - \sum (2l+1)\frac{P_l^2(y)}{2K(y,y)}\ln[P_l^2(y)] \tag{47}$$

and the corresponding Tsallis-like entropy

$$S_L^{oy}(p) = \frac{1}{p-1}\left\{1-\sum (2l+1)\left[\frac{P_l^2(y)}{2K(y,y)}\right]^p\right\}, \quad p\in R, \tag{48}$$

since

$$p_l^{oy} = \frac{P_l^2(y)}{2K(y,y)}, \quad \sum (2l+1)p_l^{oy} = 1. \tag{49}$$

D. Entropic angle–angular-momentum inequality for pure states

The angular entropy for the pure states is obtained by using definitions (1)–(3) with the angular distributions of pure states. For example, for the scattering of the spinless particles, we have

$$P(x) = \frac{2\pi}{\sigma_{\rm el}}\frac{d\sigma}{d\Omega}(x) = \left(l+\frac{1}{2}\right)P_l^2(x), \quad \int_{-1}^{1}P(x)dx = 1. \tag{50}$$

Consequently, the angular entropy S_θ is given by

$$S_\theta^l = -\int_{-1}^{+1}\left(l+\frac{1}{2}\right)P_l^2(x)\ln\left[\left(l+\frac{1}{2}\right)P_l^2(x)\right]$$
$$= \ln 2 - \ln(2l+1) - \left(l+\frac{1}{2}\right)\int_{-1}^{+1}P_l^2(x)\ln[P_l^2(x)], \tag{51}$$

while, for the pure l-state,

$$S_L^l = \ln(2l+1), \quad p_l = 1/(2l+1), \tag{52}$$

Hence for the pure state we have the state-independent angle–angular-momentum entropic inequality

$$S_\theta^l + S_L^l = \ln 2 - \left(l+\frac{1}{2}\right)\int_{-1}^{+1}P_l^2(x)\ln[P_l^2(x)]dx \geqslant \ln 2, \tag{53}$$

which is just inequality (27), since $\ln[P_l^2(x)]\leqslant 0$ for any angular momentum 1.

E. Entropic angle–angular-momentum inequality for optimal states

For optimal states we have

$$S_\theta^{oy} + S_J^{oy} = \ln 2K(y,y) - \frac{1}{2K(y,y)}\sum_{l=0}^{L}(2l+1)P_l^2(y)\ln[P_l^2(y)]$$
$$- \int_{-1}^{1}\frac{[K(x,y]^2}{K(y,y)}\ln\frac{[K(x,y]^2}{K(y,y)}dx \geqslant \ln 2 - \frac{1}{2K(y,y)}\sum_{l=0}^{L}(2l+1)P_l^2(y)\ln[P_l^2(y)]$$
$$+ \ln\left(\frac{K(y,y)}{K(1,1)}\right), \tag{54}$$

since, according to Eq. (34) and using the inequality $K(x,x)\leqslant K(1,1)$, we obtain

$$-\int_{-1}^{1}\frac{[K(x,y]^2}{K(y,y)}\ln\frac{[K(x,y]^2}{K(y,y)}dx \geqslant -\ln[K(1,1)]. \tag{55}$$

F. Optimal entropies as maximum-minimum entropies

Now we discuss in more detail the principle of minimum distance in the space of state:

$$\min\|f\|^2 \quad \text{when} \quad \frac{d\sigma}{d\Omega}(1) \ \text{is fixed.} \tag{56}$$

The unique solution of problem (56) is given by the optimal state (43) which is the particular case of the optimal state (36) when $y=1$.

Hence from Eq. (54) for $y=1$, we obtain just the inequality

$$S_\theta^{o1} + S_L^{o1} \geqslant \ln 2.$$

The optimal angular entropy S_θ^{o1} is given by

$$S_\theta^{o1} = -\int_{-1}^{1}\frac{[K(x,1]^2}{K(1,1)}\ln\frac{[K(x,1]^2}{K(1,1)}dx, \tag{57}$$

while the corresponding optimal Tsallis-like entropy $S_\theta^{o1}(q)$ can be written as

$$S_\theta^{o1}(q) = \frac{1}{q-1}\left\{1-\int_{-1}^{1}dx\left[\frac{[K(x,1]^2}{K(1,1)}\right]^q\right\}, \quad q\in R \tag{58}$$

where

$$P^{o1}(x) = \frac{[K(x,1]^2}{K(1,1)} = \frac{[\dot{P}_{L_o+1}(x)+\dot{P}_{L_o}(x)]^2}{2(L_o+1)^2}. \tag{59}$$

For the optimal angular-momentum entropies S_L^{o1} and $S_L^{o1}(q)$, we obtain

$$S_L^{o1} = \ln[2K(1,1)] = \ln(L_o+1)^2 \tag{60}$$

and

$$S_L^{o1}(q)=\frac{1}{q-1}[1-[2K(1,1)]^{1-q}]=\frac{1}{q-1}[1-[L_o+1]^{2(1-q)}], \tag{61}$$

since

$$\left\{p_l^{o1}=\frac{1}{2K(1,1)}\quad \text{for } 0\leqslant l\leqslant L_o \quad \text{and } p_l^{o1}=0 \quad \text{for l}\geqslant L_o+1\right\} \tag{62}$$

and

$$K(1,1)=\frac{1}{2}(L_o+1)^2. \tag{63}$$

Now, from comparison of the optimal distributions (62) and (26), we see that the entropic inequalities (22) and (23) can be improved up to the following most stringent entropic bounds. Indeed, solving the problems

$$\max(\min)\{S_\theta(q),S_L(q),S_{\theta L}(q)\}\quad \text{when } \sigma_{\text{el}} \quad \text{and} \quad \frac{d\sigma}{d\Omega}(1) \text{ are fixed}, \tag{64}$$

we obtain the following important bounds.

(i) The most stringent entropic bounds on the entropy $S_L(q)$, when σ_{el} and $(d\sigma/d\Omega)(1)$ are given from experiment, are

$$S_L(q)\leqslant S_L^{o1}(q) \quad \text{for } q>0, \tag{65}$$

$$S_L^{o1}(q)\leqslant S_L(q) \quad \text{for } q<0. \tag{66}$$

(ii) The most stringent entropic bounds on the entropy $S_\theta(q)$, when σ_{el} and $(d\sigma/d\Omega)(1)$ are given from experiment, are

$$S_\theta(q)\leqslant S_\theta^{o1}(q) \quad \text{for } q>0, \tag{67}$$

$$S_\theta^{o1}(q)\leqslant S_\theta(q) \quad \text{for } q<0. \tag{68}$$

(iii) The most stringent entropic bounds on $S_{\theta L}(q)$ when σ_{el} and $(d\sigma/d\Omega)(1)$ are given from experiment, are

$$S_{\theta L}(q)\leqslant S_{\theta L}^{o1}(q) \quad \text{for } q>0, \tag{69}$$

$$S_{\theta L}^{o1}(q)\leqslant S_{\theta L}(q) \quad \text{for } q<0, \tag{70}$$

where $S_\theta^{o1}(q)$, $S_L^{o1}(q)$, and $S_{\theta L}^{o1}(q)$ are given by Eqs. (57)–(61), and

$$S_{\theta L}^{o1}(q)=S_\theta^{o1}(q)+S_L^{o1}(q)+(1-q)S_\theta^{o1}(q)S_L^{o1}(q),\quad q\in R. \tag{71}$$

A general proof of the stringent entropic optimal bounds (65)–(70) can be obtained immediately by observing that these bounds are singular solutions ($\lambda_0=0$) [33] of the following extremum problems:

$$\pounds=\left\{\lambda_0 S_A(q)+\lambda_1\left[\frac{\sigma_{\text{el}}}{4\pi}-\sum\ (2l+1)|f_l|^2\right]\right.$$
$$\left.+\lambda_2\left[\frac{d\sigma}{d\Omega}(1)-\left|\sum\ (2l+1)f_l\right|^2\right]\right\}\to\text{extremum}, \tag{72}$$

where $S_A(q)\equiv\{S_\theta(q),S_L(q),S_{\theta L}(q)\}$, respectively.

Indeed, the proof that $\lambda_0=0$ in Eq. (72) is evident since we proved that there exists a solution [Eq. (43)] for the minimum distance problem (56) in the space of states when $(d\sigma/d\Omega)(1)$ is fixed. The equality holds in bounds (65)–(70) if and only if the scattering amplitude $f(x)$ of the quantum scattering (1) (see Sec. II) is given by the optimal state (43).

V. EXPERIMENTAL TESTS

A. Experimental tests of the state-independent $[\theta,L]$ entropic bounds

For a numerical investigation of our state-independent $[\theta,L]$ entropic bounds (27), (29), and (30), is interesting to calculate the entropies (6), (12), and (16) by reconstruction of the pion-nucleus scattering amplitudes using the available experimental phase-shifts [20–24] for the π^0-^{4}He, π^0-^{12}C and π^0-^{16}O, π^0-^{40}Ca scatterings. The results obtained in this way are presented in Table I and Fig. 1 as functions of the pion laboratory kinetic energy T. In the nonextensive case $p\neq 1$, we rewrote the entropic inequalities (29) and (30) in terms of the test functions $\Upsilon_{\theta L}(p)$ and $\Upsilon_{L\theta}(p)$ as

$$\Upsilon_{\theta L}(p)\equiv\frac{[1+(1-p)S_\theta(p)]^{1/2p}}{[1+(1-q)S_L(q)]^{1/2q}}\geqslant\exp\left\{\left[\frac{1-p}{2p}\right]\ln 2\right\} \tag{73}$$

and

$$\Upsilon_{L\theta}(p)\equiv\frac{[1+(1-p)S_L(p)]^{1/2p}}{[1+(1-q)S_\theta(q)]^{1/2q}}\geqslant\exp\left\{\left[\frac{1-p}{2p}\right]\ln 2\right\} \tag{74}$$

for any $1/2<p\leqslant 1$, and q is defined by $(1/2p)+(1/2q)=1$. Moreover, bounds (73) and (74) can be combined to obtain the following important $[\theta,L]$ entropic lower bound

TABLE I. The experimental values of S_θ, S_L, L_o, and L_{me}, and L calculated by using the experimental pion-nucleus phase shifts from Refs. [20–24].

Pion-nucleus scattering	T (MeV)	S_θ Eq. (6)	S_L Eq. (12)	$S_\theta+S_L$	L_{me} Eq. (69)	L_o Eq. (42)
π^0-^{4}He	25.0	0.295	1.342	1.637	0	0
	51.0	0.399	1.471	1.870	1	0
	60.0	0.414	1.507	1.921	1	0
	68.0	0.416	1.543	1.959	1	0
	75.0	0.406	1.580	1.986	1	0
	90.0	0.342	1.676	2.018	1	1
	110.0	0.152	1.836	1.988	1	1
	130.0	−0.158	2.017	1.859	1	1
	150.0	−0.444	2.139	1.695	1	2
	180.0	−0.774	2.269	1.495	2	2
	220.0	−1.037	2.406	1.369	2	2
	240.0	−1.121	2.465	1.344	2	2
	260.0	−1.167	2.504	1.337	2	3
π^0-^{12}C	30.0	0.596	1.256	1.852	0	0
	50.0	0.305	1.998	2.303	1	1
	75.6	−0.376	2.262	1.886	2	2
	80.0	−0.499	2.274	1.776	2	2
	100.0	−0.658	2.404	1.746	2	2
	148.0	−1.421	2.888	1.467	3	3
	162.0	−1.546	2.989	1.444	3	3
	226.0	−1.790	3.297	1.507	4	4
	486.0	−2.608	4.051	1.443	6	7
	584.0	−2.949	4.360	1.411	7	8
	662.0	−3.145	4.609	1.465	9	9
	672.0	−3.168	4.638	1.469	9	10
	766.0	−3.210	4.882	1.672	10	10
	870.0	−3.058	5.123	2.065	11	11
π^0-^{16}O	40.0	0.584	1.686	2.270	1	0
	50.0	0.310	2.011	2.321	1	1
	79.0	−0.772	2.479	1.708	2	2
	114.0	−1.277	2.806	1.528	3	3
	162.0	−1.756	3.216	1.460	3	4
	240.0	−2.118	3.610	1.493	5	5
	342.0	−2.423	3.916	1.494	6	6
π^0-^{40}Ca	30.5	0.567	1.329	1.896	0	0
	50.0	−0.416	2.569	2.154	2	2
	64.8	−0.978	2.786	1.808	3	3
	80.0	−1.371	2.982	1.611	3	3
	115.5	−1.728	3.381	1.653	4	4
	116.0	−1.698	3.376	1.677	4	4
	130.0	−1.925	3.534	1.609	4	5
	140.0	−2.166	3.662	1.496	5	5
	160.0	−2.322	3.816	1.494	5	6
	163.3	−2.226	3.801	1.575	5	6
	180.0	−2.402	3.938	1.536	6	6
	200.0	−2.509	4.051	1.542	6	7
	230.0	−2.586	4.195	1.609	7	7
	241.0	−2.591	4.238	1.647	7	7
	292.5	−2.739	4.458	1.719	8	8

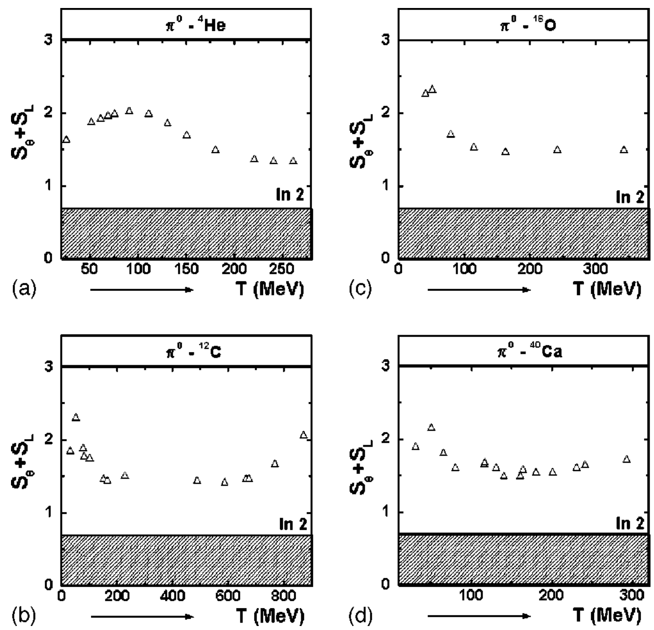

FIG. 1. (a) The experimental entropies $S_{\theta L} = S_\theta + S_L$, calculated by using Eqs. (6) and (12) and the experimental π^0-^{4}He phase shifts from Refs. [20–24], are plotted as functions of pion kinetic energy T. (b) The experimental entropies $S_{\theta L} = S_\theta + S_L$, calculated by using Eqs. (6) and (12) and the experimental π^0-^{12}C phase shifts from Refs. [20–24], are plotted as functions of pion kinetic energy T. (c) The experimental entropies $S_{\theta L} = S_\theta + S_L$, calculated by using Eqs. (6) and (12) and the experimental π^0-^{16}O phase shifts from Refs. [20–24], are plotted as functions of pion kinetic energy T. (d) The experimental entropies $S_{\theta L} = S_\theta + S_L$, calculated by using Eqs. (6) and (12) and the experimental π^0-^{40}Ca phase shifts from Refs. [20–24], are plotted as functions of pion kinetic energy T.

$$\Upsilon_{\theta L}(p)\Upsilon_{L\theta}(p) \equiv \frac{[1+(1-p)S_{\theta L}(p)]^{1/2p}}{[1+(1-q)S_{\theta L}(q)]^{1/2q}} \geqslant \exp\left\{\left[\frac{1-p}{2p}\right]\ln 4\right\} \tag{75}$$

for any $1/2 < p \leqslant 1$, and q is defined by $(1/2p)+(1/2q)=1$, where $S_{\theta L}(p)$ and $S_{\theta L}(q)$ are given by relations of form (17): $S_{\theta L}(r) = S_\theta(r) + S_L(r) + (1-r)S_\theta(r)S_L(r)$, $r=p$, and $q \in R$.

Therefore, for the nonextensive case $p \neq 1$, in Figs. 2–4 we present the experimental values of the test functions $\Upsilon_{\theta L}(p)$ and $\Upsilon_{L\theta}(p)$ for $p=0.6$ $(q=3)$ and 0.8 (or $q=4/3$), as well as for $\Upsilon_{\theta L}(p)\Upsilon_{L\theta}(p)$, for $p=0.7$ $(q=7/4)$ and 0.9 $(q=9/8)$, respectively, as functions of the pion kinetic energy T, for all the $\pi^0+{}^4\mathrm{He}\rightarrow\pi^0+{}^4\mathrm{He}$, $\pi^0+{}^{12}\mathrm{C}\rightarrow\pi^0+{}^{12}\mathrm{C}$, $\pi^0+{}^{16}\mathrm{O}\rightarrow\pi^0+{}^{16}\mathrm{O}$, $\pi^0+{}^{40}\mathrm{Ca}\rightarrow\pi^0+{}^{40}\mathrm{Ca}$ scatterings. Moreover, in Figs. 5(a)–5(d), the experimental values of entropy $S_{\theta L}$ [Eq. (16)] as well as those of the test functions $\Upsilon_{\theta L}(p)$ and $\Upsilon_{L\theta}(p)$ and $\Upsilon_{\theta L}(p)\Upsilon_{L\theta}(p)$ are presented as functions of the optimal angular momentum L_o which is obtained from the same phase shifts [20–24] by formula (46). From Figs. 1–5 we see that the $[\theta,L]$ entropic lower bound [Eq. (27)], as well as the $[p,q]$ entropic inequalities (29) and (30) in their equivalent forms [Eqs. (73)–(75)] are clearly experimentally verified with high accuracy.

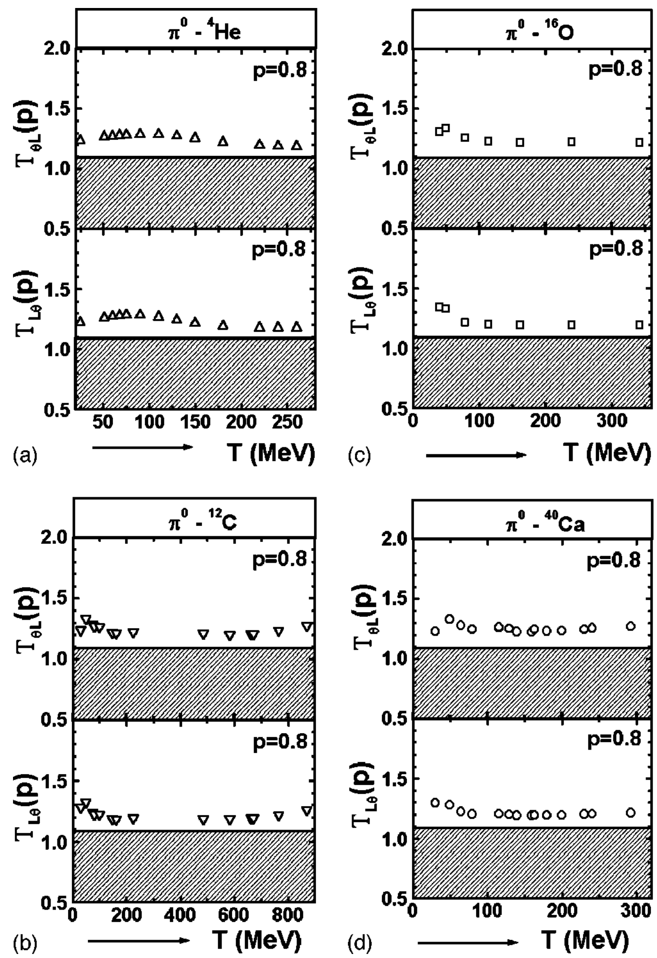

FIG. 2. (a) The experimental tests of the $[\theta,L]$ state-independent entropic lower bounds (73) and (74) for the nonextensivity index $p=0.8$, calculated by using Eqs. (6) and (12) and the experimental π^0-^{4}He phase shifts from Refs. [20–24]. (b) The experimental tests of the $[\theta,L]$ state-independent entropic lower bounds (73) and (74) for the nonextensivity index $p=0.8$, calculated by using Eqs. (6) and (12) and the experimental π^0-^{12}C phase shifts from Refs. [20–24]. (c) The experimental tests of the $[\theta,L]$ state-independent entropic lower bounds (73) and (74) for the nonextensivity index $p=0.8$, calculated by using Eqs. (6) and (12) and the experimental π^0-^{16}O phase shifts from Refs. [20–24], respectively. (d) The experimental tests of the $[\theta,L]$ state-independent entropic lower bounds (68) and (69) for the nonextensivity index $p=0.8$, calculated by using Eqs. (6) and (12) and the experimental π^0-^{40}Ca phase shifts from Refs. [20–24]. The hatched region is excluded from the physical domain due to the entropic lower bounds (68) and (69), respectively.

B. Experimental tests of principle of minimum distance in space of states

The analytic expressions of the optimal probability distributions $P^{o1}(x)$ [Eq. (59)], corresponding to the optimal state (43), are presented in Table II. The values of optimal $(S_\theta^{o1}, S_L^{o1})$ entropies for the scattering of spinless particles are obtained by numerical integration and direct from Eqs. (57) and (60), respectively. These values are presented in Table III for $0 \leqslant L_o \leqslant 25$. In Figs. 6 and 7, the experimental values of entropies S_θ and S_L as functions of the pion kinetic energy are compared with the predictions S_θ^{o1} and S_L^{o1} of the principle of minimum distance in the space of states [15].

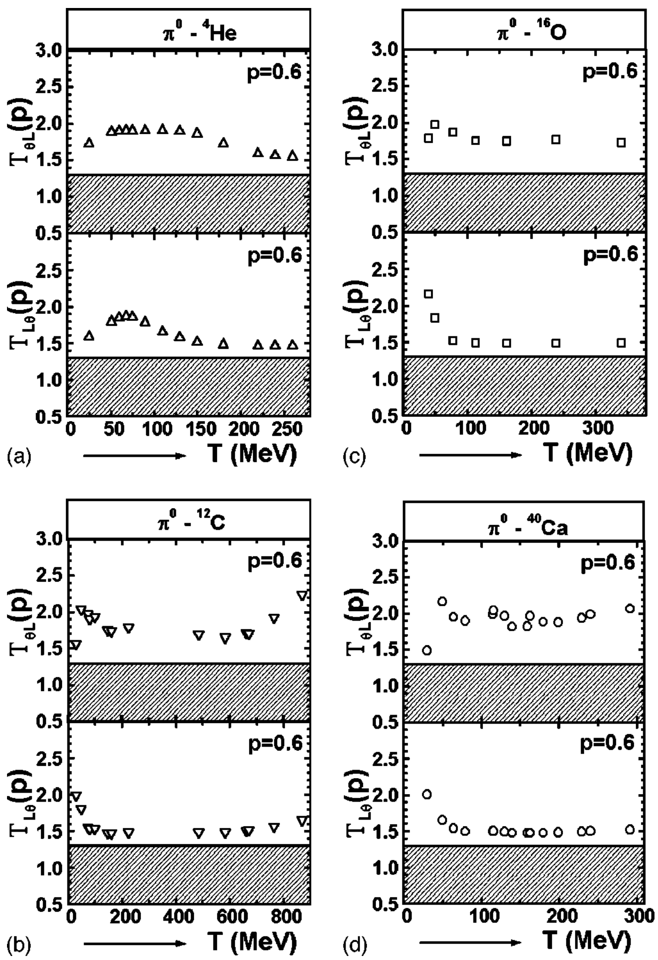

FIG. 3. (a) The experimental tests of the $[\theta,L]$ state-independent entropic lower bounds (73) and (74) for the nonextensivity index $p=0.6$, calculated by using Eqs. (6) and (12) and the experimental π^0-^{4}He phase shifts from Refs. [20–24]. (b) The experimental tests of the $[\theta,L]$ state-independent entropic lower bounds (73) and (74) for the nonextensivity index $p=0.6$, calculated by using Eqs. (6) and (12) and the experimental π^0-^{12}C phase shifts from Refs. [20–24]. (c) The experimental tests of the $[\theta,L]$ state-independent entropic lower bounds (73) and (74) for the nonextensivity index $p=0.6$, calculated by using Eqs. (6) and (12) and the experimental π^0-^{16}O phase shifts from Refs. [20–24]. (d) The experimental tests of the $[\theta,L]$ state-independent entropic lower bounds (73) and (74) for the nonextensivity index $p=0.6$, calculated by using Eqs. (6) and (12) and the experimental π^0-^{40}Ca phase shifts from Refs. [20–24].

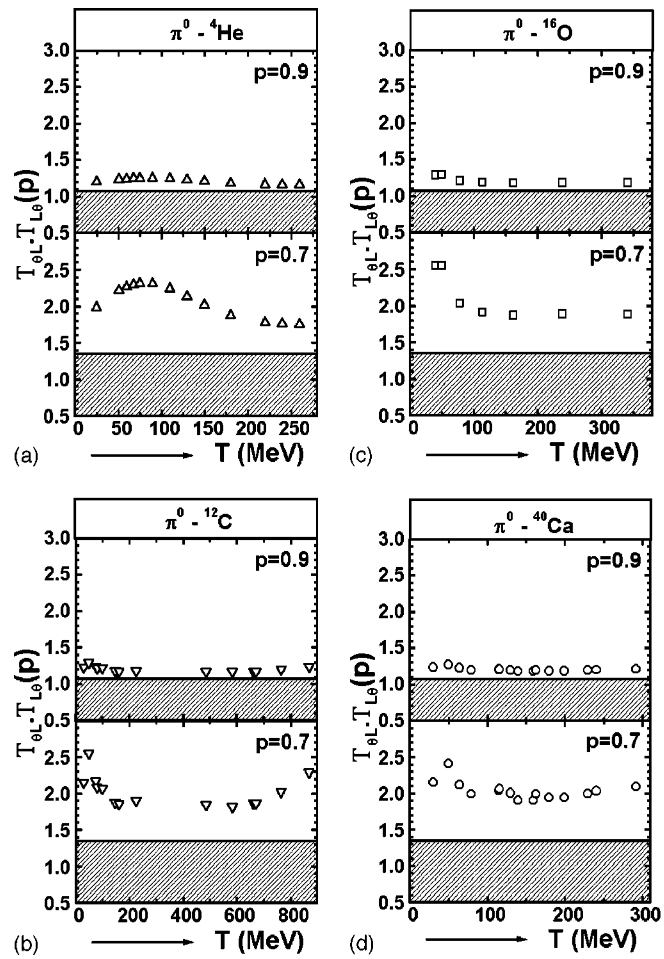

FIG. 4. (a) The experimental tests of the state-independent entropic lower bounds (75) for nonextensivity indexes $p=0.9$ and 0.7, calculated by using Eqs. (6) and (12) and the experimental π^0-^{4}He phase shifts from Refs. [20–24]. (b) The experimental tests of the state-independent entropic lower bounds (75) for nonextensivity indexes $p=0.9$ and 0.7, calculated by using Eqs. (6) and (12) and the experimental π^0-^{12}C phase shifts from Refs. [20–24]. (c) The experimental tests of the state-independent entropic lower bounds (75) for nonextensivity indexes $p=0.9$ and 0.7, calculated by using Eqs. (6) and (12) and the experimental π^0-^{16}O phase shifts from Refs. [20–24]. (d) The experimental tests of the state-independent entropic lower bounds (75) for nonextensivity indexes $p=0.9$ and 0.7, calculated by using Eqs. (6) and (12) and the experimental π^0-^{40}Ca phase shifts from Refs. [20–24].

From Figs. 6 and 7 we see that the experimental scattering entropies (S_θ,S_L) for the π^0-^{4}He, π^0-^{12}C, and π^0-^{16}O, π^0-^{40}Ca scatterings are well described (the full and dotted curves) by the optimal entropies (57) and (60). These entropies correspond to the optimal scattering state [Eq. (43)]. Clearly, the fact that the experimental entropies do not depend significantly on the atomic number A is a direct consequence of the optimal state dominance, since in this case the entropies of all hadron nuclei as a function of variable L_0 must be concentrated around the optimal values (57)–(60) given in Table III.

Now, in order to see why the experimental entropies are well described by the optimal (S_θ^{o1},S_L^{o1}) entropies (57) and (60), we observe that the entropy S_L [Eq. (12)] is similar to the Boltzmann entropy with a maximum value given by the logarithm of the number of optimal states. Indeed, from Eq. (64) we have $S_L \leqslant S_L^{o1} = \ln[2K(1,1)]$, where $2K(1,1)=\Sigma(2l+1)=(L_o+1)^2$ is the number of optimal scattering states participating at the scattering process. This result allows us to conclude that the optimal state [Eq. (43)] is the state of equilibrium of the angular-momenta channels considered as a quantum statistical ensemble. Hence, the optimal angular distribution $P^{o1}(x)$ [Eq. (59)] can be considered as a signature of this equilibrium distribution of the L channels. Also, from Figs. 6 and 7, we see that the experimental values of (S_θ,S_L) entropies for the pion-nucleus scatterings are systematically described by the optimal entropies (S_θ^{o1},S_L^{o1}) practically at all available pion kinetic energies. In this sense the results obtained here can also be considered as experi-

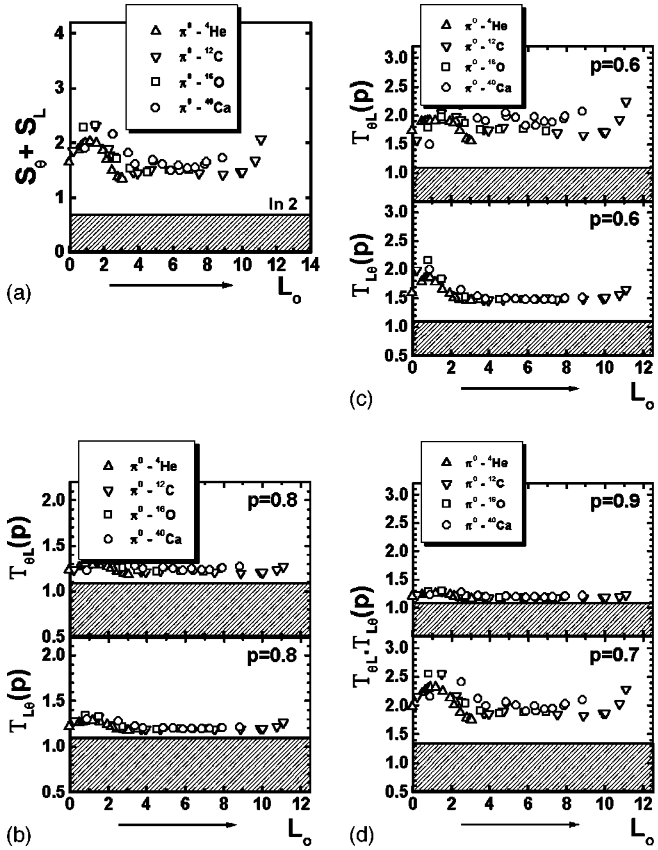

FIG. 5. (a) The scaling property of the entropies $S_{\theta L}=S_\theta+S_L$ [Eq. (16)] as a function of the optimal angular momentum L_o given by Eq. (42). (b) The scaling properties of the test functions $\Upsilon_{\theta L}$ [Eq. (73)] and $\Upsilon_{L\theta}$ [Eq. (74)] as functions of optimal angular momentum L_o [Eq. (42)] for the nonextensivity index $p=0.8$. (c) The scaling properties of the test functions $\Upsilon_{\theta L}$ [Eq. (73)] and $\Upsilon_{L\theta}$ [Eq. (74)] as functions of optimal angular momentum L_o [Eq. (42)] for the nonextensivity index $p=0.6$. (d) The scaling properties of the test functions $\Upsilon_{\theta L}\Upsilon_{L\theta}$ [Eq. (75)] as functions of optimal angular momentum L_o [Eq. (42)] for nonextensivity indexes $p=0.9$ and 0.7, respectively.

mental signatures for the validity of the principle of minimum distance in the space of scattering states, even in a crude form [15]. The extension of the optimal state analysis to the generalized nonextensive statistics case ($q\neq 1$) (see Refs. [11–13]), as well as a test of the entropic inequalities (29) and (30) and (64)–(66) for $q\neq 1$, can be obtained in similar way by using the following nonextensive optimal entropies (58) and (61).

C. Experimental test of the principle of maximum entropy

Now let us return to the maximum entropy distribution (26), and let us define and calculate $L_{\rm me}$ according to the principle of the maximum (Boltzman-like) entropy S_L [Eq. (12)]. If we consider $S_L=S_L^{\max}=\ln\{(L_{\rm me}+1)^2\}$, we have

$$L_{\rm me}=\text{integer}\times\{\exp(S_L/2)-1\}. \tag{76}$$

On the other hand, in Sec. IV we proved the general stringent upper bound [Eq. (65)] from which, for $q=1$, we obtain

$$S_L\leqslant\ln\{(L_{\rm me}+1)^2\}=S_L^{o1}=\ln\{(L_o+1)^2\}=S_L^{\max}. \tag{77}$$

TABLE II. The optimal angular distributions $P_{01}(x)$ for the scattering of spinless particles, calculated by using Eq. (59).

L_0	$P^{01}(x)=\dfrac{[K(x,1)]^2}{K(1,1)}$
0	1/2
1	$(1+3x)^2/8$
2	$(-1+2x+5x^2)^2/8$
3	$(-3-15x+15x^2+35x^3)^2/128$
4	$(3-12x-42x^2+28x^3+63x^4)^2/128$
5	$(5+35x-70x^2-210x^3+105x^4+231x^5)^2/512$
6	$(-5+30x+135x^2-180x^3-495x^4+198x^5+429x^6)^2/512$
7	$(-35-315x+945x^2+3465x^3-3465x^4-9009x^5$ $+3003x^6 6435x^7)^2/32768$
8	$(35-280x-1540x^2+3080x^3+10010x^4-8008x^5$ $-20020x^6+5720x^7+12155x^8)^2/32768$
9	$(63+693x-2772x^2-12012x^3+18018x^4+54054x^5$ $-36036x^6-87516x^7+21879x^8+46189x^9)^2/131072$
10	$(-63+630x+4095x^2-10920x^3-40950x^4+49140x^5$ $+139230x^6-79560x^7-188955x^8+41990x^9$ $+88179x^{10})^2/131072$
11	$(-231-3003x+15015x^2+75075x^3-150150x^4$ $-510510x^5+510510x^6+1385670x^7-692835x^8$ $-1616615x^9+323323x^{10}+676039x^{11})^2/2097152$
12	$(231-2772x-20790x^2+69300x^3+294525x^4-471240x^5$ $-1492260x^6+1279080x^7+3357585x^8-1492260x^9$ $-3432198x^{10}+624036x^{11}+1300075x^{12})^2/2097152$

Therefore, an experimental consistent test of the principle of maximum entropy can be obtained not only by testing the entropic upper bound (77), as is shown in Fig. 8(a), but also by a test of the equality

$$L_{\rm me}=L_o=\text{integer}\times\left[\ln\left[\frac{4\pi}{\sigma_{\rm el}}\frac{d\sigma}{d\Omega}(1)\right]-1\right]. \tag{78}$$

Indeed, using the experimental values of S_L from Table I, we calculate the values of the angular momentum $L_{\rm me}$.

TABLE III. The optimal entropies S_L^{01}, S_θ^{01}, and $S_L^{01}+S_\theta^{01}$, corresponding to different optimal angular momenta L_o, for the scattering of spinless particles.

L_0	S_θ^{o1}	S_L^{o1}	$S_\theta^{o1}+S_L^{o1}$	L_0	S_θ^{o1}	S_L^{o1}	$S_\theta^{o1}+S_L^{o1}$
0	0.693	0	0.693	13	−2.970	5.278	2.308
1	0.128	1.386	1.514	14	−3.098	5.416	2.318
2	−0.385	2.197	1.812	15	−3.219	5.545	2.326
3	−0.806	2.773	1.966	16	−3.334	5.666	2.333
4	−1.158	3.219	2.061	17	−3.442	5.781	2.339
5	−1.460	3.584	2.124	18	−3.544	5.889	2.345
6	−1.722	3.892	2.170	19	−3.641	5.992	2.351
7	−1.955	4.159	2.204	20	−3.734	6.089	2.355
8	−2.164	4.394	2.231	21	−3.823	6.182	2.360
9	−2.353	4.605	2.253	22	−3.908	6.271	2.363
10	−2.526	4.796	2.270	23	−3.989	6.356	2.367
11	−2.685	4.970	2.285	24	−4.068	6.438	2.370
12	−2.832	5.130	2.298	25	−4.143	6.516	2.373

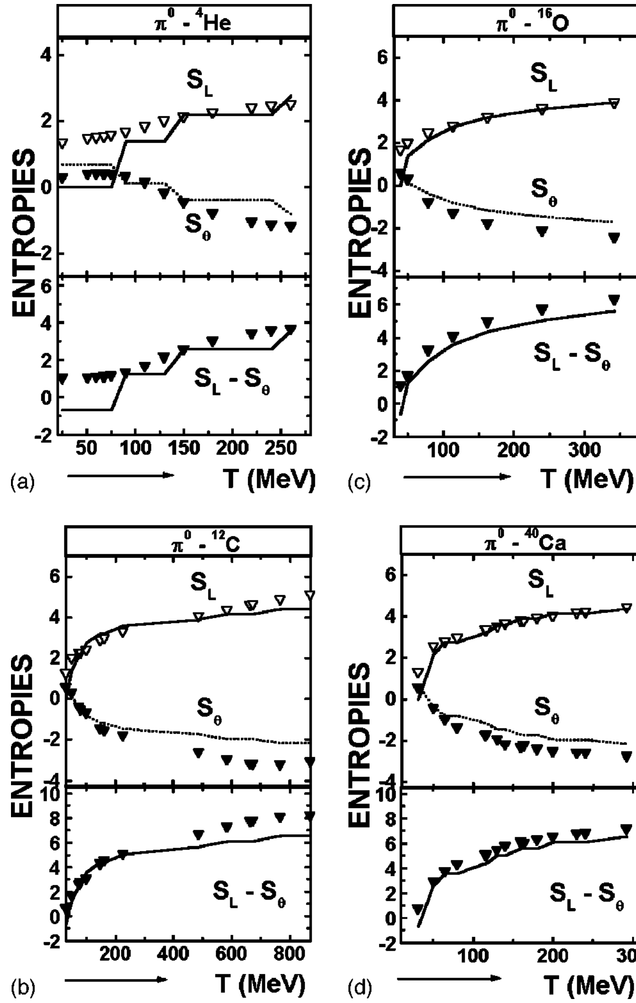

FIG. 6. (a) The experimental entropies S_θ and S_L and $S_\theta - S_L$ as functions of pion kinetic energy T, calculated by using Eqs. (6) and (12) and the experimental pion-nucleus phase shifts from Refs. [20–24]. The experimental results are compared with the optimal state predictions (57) (dotted curve) and (60) (full curve), respectively. (b) The experimental entropies S_θ and S_L and $S_\theta - S_L$ as functions of pion kinetic energy T, calculated by using Eqs. (6) and (12) and the experimental pion-nucleus phase shifts from Refs. [20–24]. The experimental results are compared with the optimal state predictions (57) (dotted curve) and (60) (full curve), respectively. (c) The experimental entropies S_θ and S_L and $S_\theta - S_L$ as functions of pion kinetic energy T, calculated by using Eqs. (6) and (12) and the experimental pion-nucleus phase shifts from Refs. [20–24]. The experimental results are compared with the optimal state predictions (dotted curves). (d) The experimental entropies S_θ and S_L and $S_\theta - S_L$ as functions of pion kinetic energy T, calculated by using Eqs. (6) and (12) and the experimental pion-nucleus phase shifts from Refs. [20–24]. The experimental results are compared with the optimal state predictions (dotted curves).

These values are compared in Table I with the experimental values of the optimal angular momentum L_o calculated from the pion-nucleus phase shifts [20–24]. As we can see from Table I, from a total number of 49 pion-nucleus experiments,

$$L_{\text{me}} = L_o \quad \text{in 34 (or 69.4\%) experiments,} \tag{79}$$

$$L_{\text{me}} = L_o - 1 \quad \text{in ten (or 20.4\%) experiments,} \tag{80}$$

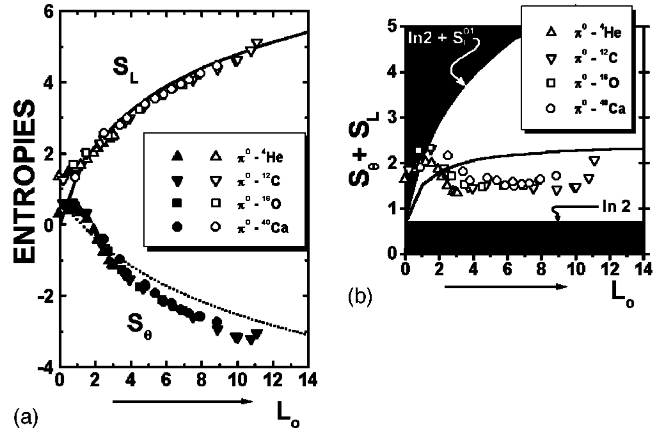

FIG. 7. (a) The scaling properties of the experimental entropies S_θ and S_L, calculated by using Eqs. (6) and (12) and the experimental pion-nucleus phase shifts [20–24], are compared with the optimal state predictions (57) (dotted curve) and (60) (full curve), respectively. (b) The scaling properties of the experimental entropies $S_\theta + S_L$, calculated by using Eqs. (6) and (12) and the experimental pion-nucleus phase shifts [20–24], are compared with the optimal state prediction (57) (full curve). The black region is excluded from the physical domain due to the entropic inequalities: $\ln 2 \leq S_\theta + S_L \leq \ln[(8\pi/\sigma_{\text{el}})(d\sigma/d\Omega)(1)]$.

and

$$L_{\text{me}} = L_o + 1 \quad \text{in five (or 10.2\%) experiments.} \tag{81}$$

Therefore, within the limit of a $\Delta L = L_{\text{me}} - L_o = 0, \pm 1$, L_{me} is described with a high accuracy by L_o. Hence, by using the available experimental pion-nucleus phase shift analyses [20–24], we illustrated the exact saturation of the entropic

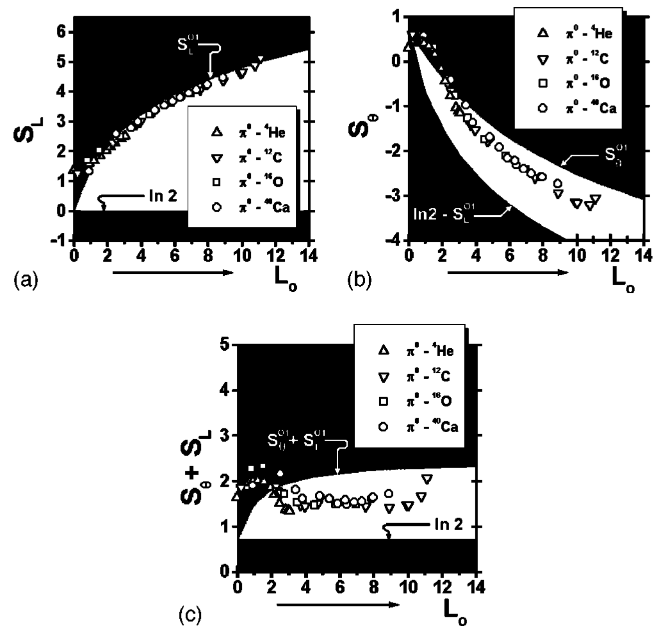

FIG. 8. (a) Experimental tests of the entropic bounds: $0 \leq S_L \leq S_L^{o1}$. The experimental data are taken from Tables I and III. (b) Experimental tests of the entropic bounds: $\ln 2 - S_L^{o1} \leq S_\theta \leq S_\theta^{o1}$. The experimental data are taken from the Tables I and III. (c) Experimental tests of the entropic bounds: $\ln 2 \leq S_\theta + S_L \leq S_\theta^{o1} + S_L^{o1}$. The experimental data are taken from Tables I and III.

upper bound [Eq. (77)] [see Fig. 8(a)]. Now in Fig. 8(b) we present an experimental test of the principle of maximum entropy S_θ. Then, we see that the upper bound

$$S_\theta \leqslant S_\theta^{o1}, \tag{82}$$

which is the particular case of the general upper bound [Eq. (67)], is also verified experimentally with high accuracy.

D. Experimental tests of the $[\theta,L]$ entropic uncertainty relations

If each of the probability entropies S_θ, S_L, and $S_{\theta L}$, defined by Eqs. (6), (12), and (16), is interpreted as natural measure of the uncertainty in the realization of the probability distributions $\{P(x), x\in[-1,+1]\}$ [Eq. (7)], $\{p_l, l\in[0,L]\}$ [Eq. (13)] and joint probability distribution $\{P(x)p_l,\ x\in[-1,+1],\ l\in[0,L]\}$, respectively, then the $[\theta,L]$ entropic lower bound [Eq. (27)] can be interpreted as state-independent $[\theta,L]$ entropic uncertainty relations. Hence, using this bound and the general entropic upper bounds [Eq. (69)], in the limit $q=1$, we obtain

$$\ln 2 \leqslant S_\theta + S_L \leqslant S_\theta^{o1} + S_L^{o1}. \tag{83}$$

In Fig. 8(c) we present an experimental verification of this important result in pion-nucleus scatterings. According to the inequality (83), the uncertainty in the realization of the joint probability distribution $\{P(x)p_l,\ x\in[-1,1]$ and $l\in[0,L]\}$ is strongly limited by

$$(\text{optimal entropic uncertainty}) \equiv S_\theta^{o1} + S_L^{o1}, \tag{84}$$

which cannot be higher than a value given by $\ln[2(L_o+1)^2] = \ln[(8\pi/\sigma_{\text{el}})(d\sigma/d\Omega)(1)]$.

The entropic uncertainty relations (see Refs. [1,9,10]) represent no generalization of the standard relation but, in principle, a formulation using the entropy as a natural measure of the uncertainty of probability distributions. If we define the statistical entropic variances as

$$\overline{\Delta\theta} = \exp(S_\theta), \quad \overline{\Delta l} = \exp(S_L), \tag{85}$$

$\overline{\Delta x}$ and $\overline{\Delta l}$, the entropic $[\theta,l]$ uncertainty relations, can be written in the form

$$2 \leqslant \overline{\Delta\theta\Delta l} \leqslant \overline{\Delta\theta}^{o1}\overline{\Delta l}^{o1} \leqslant \frac{8\pi}{\sigma_{\text{el}}}\frac{d\sigma}{d\Omega}(1). \tag{86}$$

Practical applications of the entropic uncertainty relations are considerably difficult for the reason that the entropy cannot be easily estimated in experimental practice. However, with the aid of the upper bound [Eq. (86)], we can obtain a relatively good estimation of the uncertainty of joint experimental $[\theta,L]$ probability distributions.

VI. DISCUSSIONS AND CONCLUSIONS

The results presented in this paper are valid for strong hadron-hadron, hadron-nucleus, or nucleus-nucleus scatterings for spinless hadrons and only when the electromagnetic scattering contributions are subtracted from the experimental data. However, with specific modifications of the scattering amplitude [Eq. (10)] [by adding the Coulombian amplitude $f_C(x)$ as well as by replacing each partial amplitude f_l by $f_l \exp\{i\sigma_l\}$, where σ_l are the electromagnetic phase shifts], the methods and results obtained in this paper can be extended to the general case when electromagnetic scattering contributions are not substracted. Moreover, in the case of applications to hadron-nucleus (with atomic number Z and mass number A) scattering and nucleus-nucleus scattering, a Z dependence of the experimental entropies (6) and (12) is expected to be observed only as a consequence of a violation of the charge independence of the nuclear forces, while the A dependence of these entropies can observed explicitly or is implicitly included via the optimal cutoff parameter L_o [see Eqs. (21) and (42)]. The main results obtained in this paper can be summarized as follows.

(i) The information entropies S_θ, S_L, and $S_{\theta L}$, defined by Eqs. (6), (12), and (16), are investigated in a more general form by introducing the Tsallis-like entropies [$S_\theta(q)$, $S_L(q)$, and $S_{\theta L}(q)$ for $q\in R$] for the quantum scattering of spinless particles [see definitions in Sec. II, and Eqs. (8), (14), and (17)]. The values of these entropies can be calculated by numerical integration or directly from the available model-independent amplitude analyses. Here numerical experimental values of the (S_θ, S_L) entropies for the quantum (π^0-^{4}He, π^0-^{12}C, π^0-^{16}O, and π^0-^{40}Ca) scatterings, calculated on basis of the pion-nucleus phase shifts [20–24], are presented in Table III in both extensive $q=1$ and nonextensive $q\neq 0$ cases.

(ii) The general state-independent $[\theta,L]$ entropic inequalities (29) and (30) for the Tsallis-like entropies $S_\theta(q)$, $S_L(q)$, and $S_{\theta L}(q)$, for $q\in R$, are proved in Sec. III by using the Riesz theorem (see theorem 2.8 in Ref. [19], p.102). Results of numerical tests of state-independent $[\theta,L]$ entropic lower bounds are presented in Sec. V in Figs. 1–4, while the scaling properties of the test functions are illustrated in Fig. 5.

(iii) The optimal entropies $S_\theta^{oy}(q)$ and $S_L^{oy}(q)$, corresponding to the optimal state (36), are expressed in terms of reproducing kernels in Sec. IV [see Eqs. (44)–(49)]. In particular (case $y=1$), the entropies $S_\theta^{o1}(q)$ and $S_L^{o1}(q)$, corresponding to solution (43) of the principle of minimum distance in the space of states in the form of Eq. (56) (see Ref. [15]), are given by Eqs. (57)–(63) and in numerical form in Table III. In Figs. 6 and 7, we show that the experimental values of (S_θ, S_L) entropies for pion-nucleus scatterings are systematically described by the optimal entropies $(S_\theta^{o1}, S_L^{o1})$ practical at all available pion kinetic energies. Hence these results can be considered as experimental confirmations of the validity of the principle of minimum distance in the space of scattering states even in a crude form [15]. Moreover, in Table I, we also illustrated numerically that

$$L_o = L_{\text{me}} = \exp(S_L/2) - 1 \quad \text{within} \quad \Delta L = 0, \pm 1. \tag{87}$$

In this sense, we can claim that by the validity of Eq. (87) we established a close connection between the principle of maximum entropy and the principle of minimum distance in the space of states in the form of Eq. (56).

(iv) By using the Lagrange multiplier method, in Sec. IV we proved the most stringent optimal entropic bounds (65)–(70) which are expressed in terms of optimal entropies (58) and (61). In the limiting case $q=1$, these results allow us to obtain the bounds (77) and (82), which are experimentally investigated in Figs. 8(a) and 8(b), respectively.

(v) We proved not only the state-independent entropic uncertainty [Eq. (27)], but also a general upper bound on the entropic uncertainty of the angle–angular-momentum joint distribution of the quantum scattering of spinless particles. In the particular case $q=1$, we obtain, the upper bound (83), which is expressed in terms of the optimal entropic uncertainty [Eq. (84)]. This important result is experimentally verified with high accuracy in Fig. 8(c).

It is important to note that all results of this paper can be extended to the scattering of particles with arbitrary spins by using the results of Refs. [10,16–18]. Moreover, using the RKHS methods and basic ideas contained in this paper, similar results can also be obtained for the particle production phenomena including all kinds of (strong, electromagnetic, weak, gravitational, etc.) interactions. This statement is clearly based on the following important facts: (a) The spaces of physical states are in general normed linear spaces. (b) The solutions of the minimum constrained norm (PMD-SQS) problems are expressible in terms of reproducing kernels of the RKHS of the system interacting states. (c) The optimal states, obtained via the PMD-SQS, allow us to introduce the optimal distributions of form $P(x)=[K(x,y)]^2/K(y,y)$ and $\{p_l^o\}$ optimal distributions for the corresponding Fourier components. All such results can be used for the definition of specific Tsallis-like entropies, and to obtain the entropic lower and upper bounds in terms of the optimal states derived via the principle of minimum distance in the space of states (PMD-SQS). Finally, we believe that the results obtained here are encouraging for further investigations of entropic uncertainty relations as well as the principle of minimum distance in the space of states, not only in elementary particle physics but also in other domains of science such as in genetics, biology (see, e.g., Ref. [35]), etc.

[1] M. Ohya and D. Petz, *Quantum Entropy and Its Use* (Springer-Verlag, Berlin, 1993), p. 279.
[2] H. Grad, Commun. Pure Appl. Math. **14**, 323 (1961).
[3] A. Wehrl, Rev. Mod. Phys. **50**, 221 (1978).
[4] See for example, the articles and references in R. D. Levine and M. Tribus, *The Maximum Entropy Formalism* (MIT Press, Cambridge, MA, 1979).
[5] J.F. Cyransky, J. Math. Phys. **22**, 1467 (1981).
[6] E.T. Jaynes, Phys. Rev. **106**, 620 (1957); **108**, 171 (1957).
[7] S. Kullback, *Information Theory and Statistics* (Wiley, New York, 1959), p. 37.
[8] J.E. Shore and R.W. Johnson, IEEE Trans. Inf. Theory **IT-26**, 26 (1980).
[9] I. Bialynicki-Birula and J. Mycielski, Commun. Math. Phys. **44**, 129 (1975); I. Bialynicki-Birula and J.L. Madajczuk, Phys. Lett. A **108**, 384 (1985); K. Kraus, Phys Rev. D **35**, 3070 (1987).
[10] D.B. Ion and M.L. Ion, Phys. Lett. B **352**, 155 (1995).
[11] C. Tsallis, J. Stat. Phys. **52**, 479 (1988); Phys. Lett. A **195**, 329 (1994).
[12] A.K. Rajagopal, Phys. Lett. A **205**, 32 (1995).
[13] For the most recent developments in Tsallis's entropy and/or their applications, see M. Lyra and C. Tsallis, Phys. Rev. Lett. **80**, 53 (1998), and references quoted therein.
[14] For more general nonextensive entropies, see E.P. Borges and I. Roditi, Phys. Lett. A **246**, 399 (1998).
[15] D.B. Ion, Phys. Lett. B **376**, 282 (1996).
[16] D.B. Ion and H. Scutaru, Int. J. Theor. Phys. **24**, 355 (1985).
[17] D.B. Ion, Int. J. Theor. Phys. **24**, 1217 (1985).
[18] D.B. Ion, Int. J. Theor. Phys. **25**, 1257 (1986).
[19] A. Zigmund, *Trigonometric Series* (Cambridge University Press, Cambridge, 1968), Vol. II, pp.102–104.
[20] J. Frolich, H.G. Schlaile, L. Streit, and H.F.K. Zingl, Z. Phys. A **302**, 89 (1981).
[21] O. Dumbrais, J. Frolich, U. Klein, and H.G. Schlaile, Phys. Rev. C **29**, 581 (1984).
[22] J. Frolich, H. Pilkuhn, and H.G. Schlaile, Nucl. Phys. A **415**, 399 (1984).
[23] B. Brinkmoller and H.G. Schlaile, Phys. Rev. C **48**, 1973 (1993).
[24] H.G. Schlaile, Phys. Rev. C **55**, 2584 (1997).
[25] A short version of this paper was published in D.B. Ion and M.L.D. Ion, Phys. Rev. Lett. **81**, 5714 (1998).
[26] N. Aronsjain, Proc. Cambridge Philos. Soc. **39**, 133 (1943); Trans. Am. Math. Soc. **68**, 337 (1950).
[27] S. Bergman, *The Kernel Function and Conformal Mapping*, Math. Surveys No 5. (AMS, Providence, RI, 1950).
[28] S. Bergman and M. Schiffer, *Kernel Functions and Elliptic Differential Equations in Mathematical Physics* (Academic Press, New York, 1953).
[29] A. Meschkowski, *Hilbertische Raume mit Kernfunction* (Springer, Berlin, 1962).
[30] H. S. Shapiro, *Topics in Approximation Theory*, Lectures Notes in Mathematics No. 187 (Springer, Berlin, 1971), Chap. 6.
[31] S. Saitoh, *Theory of Reproducing Kernels and its Applications* (Wiley, New York, 1988).
[32] W. Rarita and Ph. Schwed, Phys. Rev. **112**, 271 (1958).
[33] See the Lagrange multiplier rules in, e.g., V. M. Alecseev, V. M. Tihomirov, and S. V. Fomin, *Optimalinoe Upravlenie* (Nauka, Moskow, 1979), p. 47.
[34] D. J. Wilde and C. S. Beightler, *Foundations of Optimization* (Prentice-Hall, Englewood Cliffs, NJ, 1967).
[35] G.A. Parker and J. Maynard Smith, Nature (London) **348**, 27 (1990).